Laser and Particle Beams (2004), *22*, 35–40. Printed in the USA.

DOI: 10.1017/S0263034604221073

Enhanced Raman scattering of a rippled laser beam in a magnetized collisional plasma

NARESHPAL SINGH SAINI, AND TARSEM SINGH GILL
Department of Physics, Guru Nanak Dev University, Amritsar, India

(RECEIVED 10 December 2002; ACCEPTED 25 May 2003)

Abstract

In the laser–plasma interaction experiments, self-focusing and filamentation affect quite a large number of other parametric processes including stimulated scattering processes. Nonlinearity considered in the present problem is the collisional type. The coupling between the main beam, ripple, and excited electron plasma wave is strong. Authors have investigated the growing interaction of a rippled laser beam with an electron plasma wave leading to enhanced Raman scattering. An expression for scattered power is derived and the effect of the externally applied magnetic field on the enhancement of scattered power is observed. From computational results, it is observed that the effect of increased intensity of the main beam leads to suppression of power associated with the Raman scattered wave.

Keywords: Collisional plasma; Coupling; Raman scattering; Rippled laser beam

1. INTRODUCTION

The stimulated scattering processes and filamentation of laser light remain key issues of laser–plasma interactions relevant to inertial confinement fusion (ICF). In the stimulated Raman scattering (SRS), incident light on plasma is converted into an electron plasma wave and low-frequency scattered photons. Two major problems associated with SRS are as follows:

1. First, the scattered wave represents a substantial amount of wasted energy as SRS yields are as high 25%.
2. Second, the large amplitude plasma wave produces superthermal electrons that penetrate and preheat the target core, thereby preventing the efficient implosion.

Furthermore, self-focusing and filamentation are other basic issues to be resolved for the success of ICF. In the laser–plasma experiments, the filamentary structure created in underdense plasma undergoes self-focusing by the same mechanism as that of the main beam. The origin of filamentation instability may be attributed to a small-scale intensity spike associated with the main beam. Particularly in the hot spots of the laser beam, self-focusing or filamentation grows unstably through a feedback mechanism of increased electron thermal pressure via ponderomotive force or other nonlinear mechanisms. The resulting redistribution of the carriers leads to an increased index of refraction which further results in concentration of intensity in the regions of hot spots. Thus, perturbation grows at the cost of the main beam and the overall effect is distortion of propagation characteristics, inefficient laser–energy coupling to the target, and a loss of symmetry of the energy deposition, leading to hydrodynamical instabilities of the target.

In theoretical studies, many interesting properties of stimulated back scattering, self-focusing, and filamentation have been carried out separately, ignoring interplay among them. There is also no reason to separate the evolution of these instabilities in the nonlinear regime where they coexist and affect each other (Amin *et al.*, 1993). It is important to investigate and understand interplay among various instabilities. Liu and Tripathi (1995) have recently studied the thermal effects on coupled self-focusing and Raman scattering of laser beams in a self-focused plasma channel. In light of considerable current interest in self-focusing and SRS (Short & Simon, 1998; Russell *et al.*, 1999; Fuchs *et al.*, 2000) and in view of earlier work (Sodha *et al.*, 1981; Singh *et al.*, 1987; Saini & Gill, 2002), we here study the growing interaction of a rippled laser beam with a electron plasma wave mode leading to enhanced Raman scattering for magnetized collisional plasma. This model was used earlier in other nonlinear excitation processes (Singh & Singh, 1990, 1999; Saini & Gill, 2002). This model takes care of whole

Address correspondence and reprint requests to: Nareshpal Singh Saini, Department of Physics, Guru Nanak Dev University, Amritsar–143005, India. E-mail: nssaini@yahoo.com

beam self-focusing, small-scale self-focusing, and their combined effect on the excitation of a plasma wave that consequently affects the stimulated scattering processes. Thus, it is important to investigate nonlinear coupling of self-focusing, filamentation, and SRS. In the case of magnetized collisional plasma the nonlinearity arises due nonuniform heating of the carriers along the wave front, and the redistribution of carriers is affected by the change in the static magnetic field.

2. SOLUTION OF THE WAVE EQUATION

Consider the propagation of a laser beam of angular frequency ω_0 in a homogeneous magnetized plasma along the externally applied static magnetic field $\mathbf{B}_0$ coincident with the z-axis. The initial intensity distributions of the main beam and the ripple are given by

$$\mathbf{E}_{0\pm}\cdot\mathbf{E}_{0\pm}^{*} = E_{00}^2 \exp\left(-\frac{r^2}{r_0^2}\right) \tag{1}$$

and

$$\mathbf{E}_{1\pm}\cdot\mathbf{E}_{1\pm}^{*} = E_{100}^2 \left(\frac{r}{r_{10}}\right)^{2n} \exp\left(-\frac{r^2}{r_{10}^2}\right), \tag{2}$$

respectively. Here n is a positive number, $r^2 = x^2 + y^2$, and r_{10} is the width of the ripple. As n increases, the maximum $(r_{\max} = r_{10} n^{1/2})$ of the ripple shifts away from the axis. The ripple is symmetrically superimposed on the main Gaussian beam. In collisional magnetoplasma, when $\nu^2 \ll (\omega_0 - \omega_c)^2$, we obtain a modified carrier density that is given by (Sodha *et al.*, 1983)

$$N_{0e} = N_0\left[1 - \frac{\dfrac{8}{3}\alpha_0 \dfrac{M}{m} \dfrac{\mathbf{E}_{\mathbf{t}\pm}\cdot\mathbf{E}_{\mathbf{t}\pm}^{*}}{(1-\omega_c/\omega_0)^2}}{\left(2 + \dfrac{8}{3}\alpha_0 \dfrac{M}{m} \dfrac{\mathbf{E}_{\mathbf{t}\pm}\cdot\mathbf{E}_{\mathbf{t}\pm}^{*}}{(1-\omega_c/\omega_0)^2}\right)}\right], \tag{3}$$

where $\alpha_0 = e^2/(16k_B T_0 m\omega_0^2)$, $\mathbf{E}_{\mathbf{t}\pm} = \mathbf{E}_{\mathbf{0}\pm} + \mathbf{E}_{\mathbf{1}\pm}$ and $\varepsilon_{\pm} = \varepsilon_{0\pm} + \Phi_{\pm}(\mathbf{E}_{\mathbf{t}\pm} + \cdot\mathbf{E}_{\mathbf{t}\pm}^{*})$. In WKB approximation, we can write the wave equation for the total electric vector, which leads to the following equations (for one mode) for the main beam and the ripple:

$$\frac{\partial^2 \mathbf{E}_{\mathbf{0}\pm}}{\partial z^2} + \frac{1}{2}\left(1 + \frac{\varepsilon_{0+}}{\varepsilon_{0zz}}\right)\left(\frac{\partial^2}{\partial x^2} + \frac{\partial^2}{\partial y^2}\right)\mathbf{E}_{\mathbf{0}+} + \frac{\omega_0^2}{c^2}[\varepsilon_{0+} + \Phi_{+}(\mathbf{E}_{\mathbf{0}+}\cdot\mathbf{E}_{\mathbf{0}+}^{*})]\mathbf{E}_{\mathbf{0}+} = 0 \tag{4}$$

and

$$\frac{\partial^2 \mathbf{E}_{\mathbf{1}+}}{\partial z^2} + \frac{1}{2}\left(1 + \frac{\varepsilon_{0+}}{\varepsilon_{0zz}}\right)\left(\frac{\partial^2}{\partial x^2} + \frac{\partial^2}{\partial y^2}\right)\mathbf{E}_{\mathbf{1}+} + \frac{\omega_0^2}{c^2}[\varepsilon_{0+} + \Phi_{+}(\mathbf{E}_{\mathbf{t}+}\cdot\mathbf{E}_{\mathbf{t}+}^{*})]\mathbf{E}_{\mathbf{1}+} + \frac{\omega_0^2}{c^2}[\Phi_{+}(\mathbf{E}_{\mathbf{t}+}\cdot\mathbf{E}_{\mathbf{t}+}^{*}) - \Phi_{+}(\mathbf{E}_{\mathbf{0}+}\cdot\mathbf{E}_{\mathbf{0}+}^{*})]\mathbf{E}_{\mathbf{0}+} = 0. \tag{5}$$

For the sake of simplicity, we shall drop the subscript + from subsequent analysis. Following Akhmanov *et al.* (1968) and Sodha *et al.* (1976), the solutions of Eqs. (4) and (5) are obtained and the dimensionless beam width parameters of main beam f_0 and ripple f_1 are governed by the following equations:

$$\frac{d^2 f_0}{dz^2} = \frac{\left(1 + \dfrac{\varepsilon_0}{\varepsilon_{0zz}}\right)^2}{4k_0^2 r_0^4 f_0^3} - \frac{\left(1 + \dfrac{\varepsilon_0}{\varepsilon_{0zz}}\right)}{2\varepsilon_0 r_0^2 f_0^2 (1-\omega_c/\omega_0)^3}\alpha E_{00}^2 \frac{\omega_p^2}{\omega_0^2} \times \left[\frac{1}{2 + \dfrac{\alpha E_{00}^2}{(1-\omega_c/\omega_0)^2 f_0^2}} - \frac{\alpha E_{00}^2}{f_0^2(1-\omega_c/\omega_0)^2\left(2 + \dfrac{\alpha E_{00}^2}{(1-\omega_c/\omega_0)^2 f_0^2}\right)^2}\right] \tag{6}$$

$$\begin{aligned}\frac{d^2 f_1}{dz^2} = {}& \frac{c^2\left(1 + \dfrac{\varepsilon_0}{\varepsilon_{0zz}}\right)^2}{4\omega_0^2 r_{10}^4 f_1^3 \varepsilon_0} - \frac{\left(1 + \dfrac{\varepsilon_0}{\varepsilon_{0zz}}\right) f_1 \alpha E_{00}^2 \omega_p^2}{2\varepsilon_0 \omega_0^2 r_0^2 (1-\omega_c/\omega_0)^3} \\ & \times \left[\frac{T_2}{\left(2 + \dfrac{\alpha E_{00}^2 T_3}{(1-\omega_c/\omega_0)^2}\right)} \times \left(1 - \frac{\alpha E_{00}^2 T_3}{(1-\omega_c/\omega_0)^2\left(2 + \dfrac{\alpha E_{00}^2 T_3}{(1-\omega_c/\omega_0)^2}\right)}\right) \right. \\ & + \frac{2\cos^2\phi_p T_4}{f_0^4} \times \left(\frac{(2 + 2\alpha E_{00}^2 T_4)}{\left[2 + \dfrac{\alpha E_{00}^2 T_4}{f_0^2(1-\omega_c/\omega_0)^2}\right]^2} \right. \\ & \left.\left. - \frac{2(\alpha E_{00}^2)^2 T_4^2}{(1-\omega_c/\omega_0)^2 f_0^4 \left[2 + \dfrac{\alpha E_{00}^2 T_4}{f_0^2(1-\omega_c/\omega_0)^2}\right]^3}\right)\right],\end{aligned} \tag{7}$$

https://doi.org/10.1017/S0263034604221073 Published online by Cambridge University Press

where

$$T_2 = \frac{\exp\left(-\dfrac{r_{10}^2 f_1^2 n}{r_0^2 f_0^2}\right)}{f_0^4} + \frac{\cos\phi_p n^{n/2}(E_{100}/E_{00})}{f_0^3 f_1} \times \exp\left(-\int_0^z k_i\,dz\right)\exp\left(-\frac{n}{2} - \frac{r_{10}^2 f_1^2 n}{2r_0^2 f_0^2}\right)$$

$$T_3 = \frac{\exp\left(-\dfrac{r_{10}^2 f_1^2 n}{r_0^2 f_0^2}\right)}{f_0^2} + \frac{2\cos\phi_p n^{n/2}(E_{100}/E_{00})}{f_0 f_1} \times \exp\left(-\frac{n}{2} - \frac{r_{10}^2 f_1^2 n}{2r_0^2 f_0^2}\right)$$

$$T_4 = \exp\left(-\frac{r_{10}^2 f_1^2 n}{r_0^2 f_0^2}\right), \tag{8}$$

with

$$\varepsilon_0 = 1 - \frac{\omega_p^2/\omega_0^2}{(1 \mp \omega_c/\omega_0)},$$

$$\varepsilon_{0zz} = 1 - \omega_p^2/\omega_0^2 \qquad \text{and} \qquad \alpha = (8/3)(\mathrm{M/m})\alpha_0.$$

The initial conditions on f_0 and f_1 for a plane wave front, are $df_0/dz = 0 = df_1/dz$ and $f_0 = 1 = f_1$ at $z = 0$. The expression for the growth rate of the ripple can be written as

$$k_i \cong \frac{1}{2}\frac{\omega_0^2}{c^2}\frac{1}{k_0}\frac{1}{f_0^2}\frac{\omega_p^2}{\omega_0^2}\frac{\alpha E_{00}^2}{(1-\omega_c/\omega_0)^3}\sin(2\phi_p)T_5, \tag{9}$$

with

$$T_5 = \frac{1}{2 + \dfrac{\alpha E_{00}^2}{f_0^2(1-\omega_c/\omega_0)^2}} - \frac{\alpha E_{00}^2}{f_0^2(1-\omega_c/\omega_0)^2}\frac{1}{\left(2 + \dfrac{\alpha E_{00}^2}{f_0^2(1-\omega_c/\omega_0)^2}\right)^2}. \tag{10}$$

3. EXCITATION OF ELECTRON PLASMA WAVE (EPW)

A weak electron plasma wave is nonlinearly coupled to a rippled laser beam via modified background density. Thus, self-focusing of the main beam, ripple, and the dynamics of growth of the ripple, all substantially affect the excitation of the plasma wave. Using perturbation analysis and Sodha *et al.* (1981), it is possible to show the excitation of EPW by the following equation:

$$\frac{d^2 n'}{dt^2} - v_{th}^2\nabla^2 n' + \omega_{pe}^2\frac{N_{0e}}{N_0}n' = 0. \tag{11}$$

Using WKB and paraxial ray (PR) approximations and following the approach developed by Akhmanov *et al.* (1968) and Sodha *et al.* (1976), the dimensionless beam width parameter f_p of the plasma wave is governed by the following equation:

$$\frac{d^2 f_p}{dz^2} = \frac{1}{k^2 a_0^4 f_p^3} - \frac{\omega_p^2 f_p}{k^2 v_{th}^2(1-\omega_c/\omega_0)^2} \times \left(\frac{\sqrt{2}\alpha}{2 + \dfrac{\alpha}{(1-\omega_c/\omega_0)^2}\mathbf{E_t}\cdot\mathbf{E_t^*}}\right)^2 \times \left[\frac{E_{00}E_{100}}{f_0 f_1}\cos(\phi_p)n^{n/2}\exp\left(-\int_0^z k_i\,dz\right)\frac{1}{r_0^2 f_0^2} \times \exp\left(-\frac{n}{2} - \frac{r_{10}^2 f_1^2 n}{r_0^2 f_0^2}\right) + \frac{E_{00}^2}{r_0^2 f_0^4}\exp\left(-\frac{r_{10}^2 f_1^2 n}{r_0^2 f_0^2}\right)\right]. \tag{12}$$

4. ENHANCED RAMAN SCATTERING

Interaction of the incident pump (ω_0, $\mathbf{k_0}$) with the electron plasma wave (ω, $\mathbf{k}$) leads to generation of a scattered wave (ω_S, $\mathbf{k_S}$). Using the approach in Singh and Salimullah (1987), the wave equation for the scattered electric field can be derived as

$$\nabla^2\mathbf{E_S} + \frac{\omega_S^2}{c^2}\left[1 - \frac{\omega_p^2 N_{0e}}{\omega_S^2 N_0}\right]\mathbf{E_S} = \frac{\omega_p^2\omega_S n'^*}{2c^2\omega_0 N_0}\mathbf{E_0}. \tag{13}$$

We assume the following solution for **Es**:

$$\mathbf{E_S} = \mathbf{E'_S}(x,y,z)\exp(\iota k_S z) + \mathbf{E''_S}(x,y,z)\exp(-\iota k_{S1} z), \tag{14}$$

where

$$k_S^2 = \frac{\omega_S^2}{c^2}\left(1 - \frac{\omega_p^2}{\omega_S^2}\right), \quad k_{S1} = k_0 - k.$$

Equation (13) can be solved following the procedure of Akhmanov *et al.* (1968), Sodha *et al.* (1976), and Singh and Salimullah (1987). The dimensionless beam width parameter f_s of the scattered beam is governed by the following equation:

https://doi.org/10.1017/S0263034604221073 Published online by Cambridge University Press

$$\frac{d^2 f_S}{dz^2} = \frac{1}{k_S^2 a_S^4 f_S^3} - \frac{\omega_p^2 f_S}{k_S^2 c^2 (1-\omega_c/\omega_0)^2}$$
$$\times \left(\frac{\sqrt{2}\alpha}{2 + \frac{\alpha}{(1-\omega_c/\omega_0)^2} \mathbf{E_t}\cdot\mathbf{E_t^*}} \right)^2$$
$$\times \left[\frac{E_{00}E_{100}}{f_0 f_1} \cos(\phi_p) n^{n/2} \exp\left(-\int_0^z k_i\, dz\right) \frac{1}{r_0^2 f_0^2} \right.$$
$$\left. \times \exp\left(-\frac{n}{2} - \frac{r_{10}^2 f_1^2 n}{r_0^2 f_0^2}\right) + \frac{E_{00}^2}{r_0^2 f_0^4} \exp\left(-\frac{r_{10}^2 f_1^2 n}{r_0^2 f_0^2}\right)\right]. \tag{15}$$

Finally, the total scattered power of the scattered laser beam is given by (Singh, 1981)

$$P_S = \frac{c}{32} \varepsilon_S^{1/2} \left(\frac{E_{00} n_{00} \omega_p^2}{N_0 c^2}\right)^2 \frac{\omega_S^2}{\omega_0^2}$$
$$\times \left[\left(\frac{f_S}{f_0 f_p}\right)^2_{z=z_c} \frac{a_S^2}{D_{r1}^2(0)} \exp(-2k_d z_c) \frac{\cos^2(k_0 - k) z_c}{\cos^2(k_S z_c)} \right.$$
$$+ \frac{1}{f_p^2 f_0^2 D_{r1}^2} \exp(-2k_d z) \frac{1}{\left(\frac{1}{r_0^2 f_0^2} + \frac{1}{a_0^2 f_p^2}\right)}$$
$$- 4\left(\frac{f_S}{f_0 f_p}\right)_{z=z_c} \frac{1}{f_0 f_p f_S} \frac{\exp(-k_d z_c - k_d z)}{D_{r1} D_{r1}(0)}$$
$$\left. \times \frac{\cos(k_0 - k) z_c}{\cos(k_S z_c)} \frac{\cos Q_1}{(1/(r_0^2 f_0^2) + 1/(a_0^2 f_p^2) + 1/(a_S^2 f_S^2))} \right], \tag{16}$$

where $Q_1 = k_S S_S + k_0 S_0 - k S_P + (k_S + k_{S1}) z$ and

$$D_{r1} = (k_0 - k)^2 - \frac{\omega_S^2}{c^2}\left[1 - \frac{\omega_p^2 N_{0e}}{\omega_S^2 N_0}\right], \tag{17}$$

with $D_{r1} = D_{r1}(0)$ at $z = z_c$ and $r = 0$.

5. DISCUSSION

It is obvious from the present analysis that because of the coupling between the main beam and ripple, the ripple can grow/decay inside the plasma and the growth rate (k_i) is given by (9). As is apparent from this expression, it depends on pump and plasma parameters. Besides that, it depends on the angle between the ripple and main beam and the externally applied magnetic field. We have chosen the following set of parameters for numerical calculations:

$$\left(\frac{r_0 \omega_p}{c}\right)^2 = 20, \quad \frac{\omega_p}{\omega_0} = 0.5, \quad \omega_0 = 1.778 \times 10^{14} \text{ rad/s},$$
$$n = 1.0, \quad 2\phi_p = \frac{\pi}{2}, \quad \frac{r_{10}^2}{r_0^2} = 0.3, \quad \frac{r_{10}}{a_0} = 0.8,$$
$$\frac{r_{10}}{a_s} = 0.4, \quad aE_{00}^2 = 4.0, \quad \frac{\omega_c}{\omega_0} = 0.3.$$

Equation (6) is a second-order, nonlinear, ordinary differential equation, governing the focusing/defocusing of the main beam as it propagates through the plasma. If the first term is large in comparison to the second, then diffraction dominates over the nonlinear phenomenon, leading to defocusing of the beam. The situation is quite the opposite when the second term is larger than the first and self-focusing of the beam is observed. It must be mentioned that relative magnitudes of these terms keep on changing with the distance of propagation. We have solved all equations numerically using the Runge–Kutta method.

Equation (7) governs the dynamics of the ripple intensity with the distance of propagation. As is apparent from the form of (7), its structure is similar to (6) for f_0 and it is also a nonlinear, ordinary differential equation. Besides that, the beam width parameter f_0 of the main beam appears in this equation for f_1. Apparently, the focusing of the main beam drastically affects the focusing of the ripple.

In Figure 1, we have plotted beam width parameter f_1 as a function of the normalized distance of propagation $\xi(=zc/\omega_0 r_{10}^2)$ for two values of n, with $\alpha E_{00}^2 = 4.0$, $\omega_c/\omega_0 = 0.6$, and the other chosen parameters are the same. Curve 1 is for $n = 1$, whereas Curve 2 is for $n = 2$. The smaller the value of n, the larger oscillatory self-defocusing/focusing is observed.

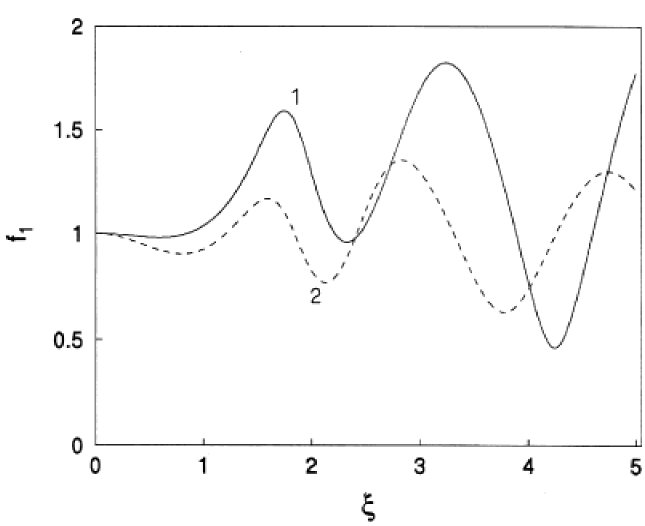

Fig. 1. Beam width parameter f_1 of the ripple plotted against the normalized distance of propagation $\xi(= zc/\omega_0 r_{10}^2)$ in a collisional magnetoplasma for the chosen set of parameters. Curve 1 is for $n = 1.0$ and Curve 2 for $n = 2.0$.

https://doi.org/10.1017/S0263034604221073 Published online by Cambridge University Press

Figure 2 depicts the variation of the beam width parameter f_p of the excited plasma wave for the above mentioned set of parameters and for three values of the magnetic field. Curve 1 is for $\omega_c/\omega_0 = 0.0$, Curve 2 is for $\omega_c/\omega_0 = 0.3$, and Curve 3 is for $\omega_c/\omega_0 = 0.6$. It is observed that an increase in the magnetic field not only slows down the self-focusing, but also leads to oscillatory defocusing/focusing of the beam. This is due to reduced nonlinear coupling of the electron plasma wave to the rippled laser beam with an increasing magnetic field.

The excited electron plasma wave is so strong that it nonlinearly interacts with the main beam, leading to a Raman-scattered wave. Equation (15) determines the dynamics of self-focusing of the scattered wave as a function of ξ. We observe here that f_0, f_1, and f_p jointly determine the focusing/defocusing of the scattered wave and consequently the variation of the normalized scattered power P $(= P_S/P_0)$ as a function of ξ. In Figure 3, Curve 1 is for $\omega_c/\omega_0 = 0.0$, Curve 2 is for $\omega_c/\omega_0 = 0.3$, and Curve 3 is for $\omega_c/\omega_0 = 0.6$. For lower values of the magnetic field, however, scattered power depends on focusing of f_0, f_1, and f_p as well as f_s, but is peaked dominantly by f_1. However, a low magnetic field suppresses the scattered power. But when the magnetic field is increased to $\omega_c/\omega_0 = 0.6$, normalized scattered power P reaches as high as 8% with the distance of propagation. Moreover, scattered power P is dominantly determined by focusing of the main beam and plasma wave as well as the scattered wave. Besides other parameters, the ripple dynamics and magnetic field play a significant role for scattered power.

Figure 4 displays the normalized scattered power as a function of ξ for three different values of intensity parameter and a fixed value of the magnetic field ($\omega_c/\omega_0 = 0.6$).

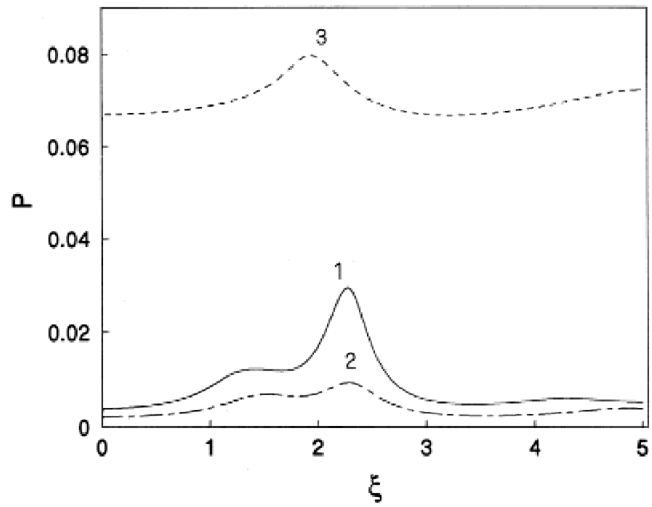

Fig. 3. Variation of the normalized power $P(= P_S/P_0)$ with the normalized distance of propagation ξ for different values of the magnetic field; the other parameters are the same. Curve 1 is for $\omega_c/\omega_0 = 0$, Curve 2 corresponds to $\omega_c/\omega_0 = 0.3$, and Curve 3 corresponds to $\omega_c/\omega_0 = 0.6$.

Curve 1 is for $\alpha E_{00}^2 = 4.0$, Curve 2 is $\alpha E_{00}^2 = 5.0$, and Curve 3 is for $\alpha E_{00}^2 = 6.0$. The following observations are made:

1. Scattered power is highest for the low intensity parameter.
2. An increase in intensity suppresses the scattered power.
3. There is a shift in the maximum scattered power with ξ for different values of the intensity parameter. It is due to phase mixing of various terms in the expression for scattered power as these terms keep on varying with ξ.

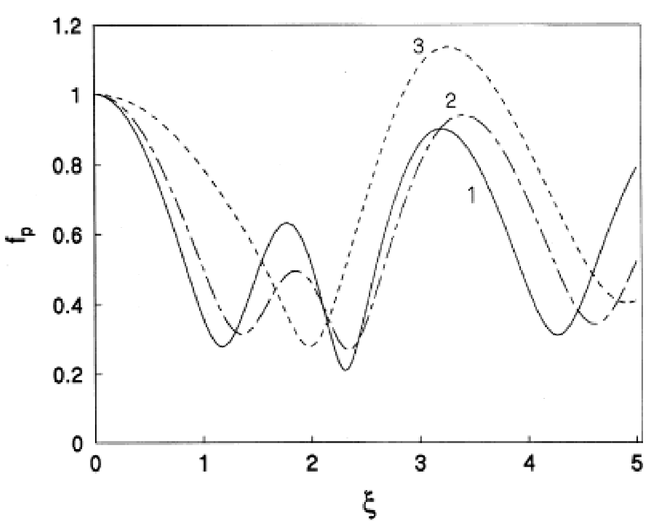

Fig. 2. Beam width parameter f_p of the excited plasma wave plotted against the normalized distance of propagation ξ for different values of the magnetic field; the other parameters are the same. Curve 1 is for $\omega_c/\omega_0 = 0$, Curve 2 corresponds to $\omega_c/\omega_0 = 0.3$, and Curve 3 corresponds to $\omega_c/\omega_0 = 0.6$.

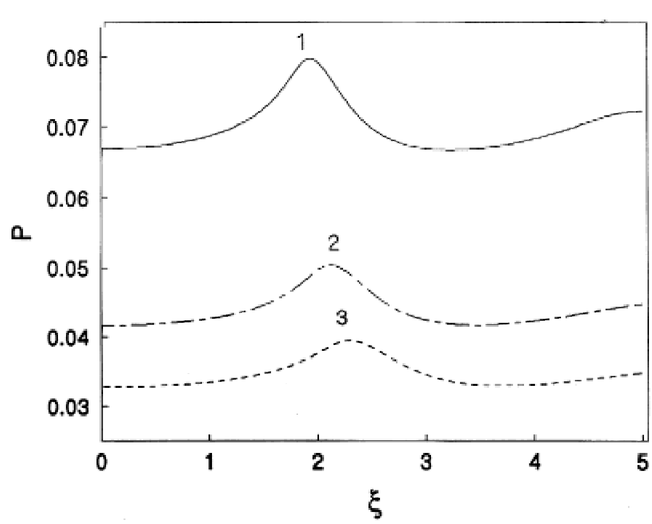

Fig. 4. Variation of the normalized power $P(= P_S/P_0)$ with the normalized distance of propagation ξ for different values of intensity with $\omega_c/\omega_0 = 0.6$; the other parameters are the same. Curve 1 is for $\alpha E_{00}^2 = 4.0$, Curve 2 is $\alpha E_{00}^2 = 5.0$, and Curve 3 is for $\alpha E_{00}^2 = 6.0$.

https://doi.org/10.1017/S0263034604221073 Published online by Cambridge University Press

6. CONCLUSIONS

The introduction of a magnetic field weakens the nonlinear term, leading to decreased self-focusing of the ripple. This behavior becomes more succinct as is obvious from Figure 1 and Figure 2. Further, the effect of an increasing magnetic field leads to a decrease in coupling of EPW to the rippled laser beam. This behavior is quite opposite to the one observed earlier (Saini & Gill, 2002). We also obtain high scattered power for low intensity and wiggles in the scattered power are smoothed. This behavior is also contrary to the one observed earlier (Saini & Gill, 2002). Thus, the magnetic field plays a crucial role in the dynamics of the rippled laser beam propagation in plasma.

REFERENCES

Akhmanov, S.A., Sukhorbikov, A.P. & Khokhlov, R.V. (1968). *Sov. Phys. Usp.* **10**, 609.

Amin, M.R., Capjack, C.E., Frycz, P., Rozmus, W. & Tikhonchuk, V.T. (1993). Two-dimensional studies of stimulated Brillouin scattering, filamentation, and self-focusing instabilities of laser light in plasmas. *Phys. Fluids* **5**, 3748–3764.

Fuchs, J., Labaune, C., Depierreux, S., Tikhonchuk, V.T. & Baldis, H.A. (2000). Stimulated Brillouin and Raman scattering from a randomized laser beam in large inhomogeneous collisional plasmas. *I. Experiment Phys. Plasmas* **7**, 4659–4668.

Liu, C.S. & Tripathi, V.K. (1995). Thermal effects on coupled self-focusing and Raman scattering of a laser in a self-consistent plasma channel. *Phys. Plasmas* **2**, 3111–3114.

Russell, D.A., DuBois, D.F. & Rose, H.A. (1999). Nonlinear saturation of stimulated Raman scattering in laser hot spots. *Phys. Plasmas* **6**, 1294–1317.

Saini, N.S. & Gill, T.S. (2002). Advances in contemporary physics & energy (supplement) New Delhi, India: Allied Publishers Pvt. Ltd., 111–127.

Short, R. W. & Simon, A. (1998). Collisionless damping of localized plasma waves in laser-produced plasmas and application to stimulated Raman scattering in filaments. *Phys. Plasmas* **5**, 4134–4143.

Singh, A. & Singh, T. (1990). The effect of a static magnetic field on the growth of a rippled electromagnetic beam. *J. Plasma Phys.* **43**, 465–474.

Singh, N. & Singh, T. (1999). Growth of laser ripple in a collisional magnetoplasma and its effect on plasma wave excitation. *J. Plasma Fusion Res.* **2**, 423–426

Singh, T. (1981). Excitation of waves and scattering phenomena in Plasmas, PhD Thesis, Indian Institute of Technology Delhi. New Delhi: India.

Singh, T. & Salimullah, M. (1987). Nonlinear Interaction of a Gaussian EM Beam with an Electrostatic Upper Hybrid Wave: Stimulated Raman Scattering. *IL Nuovo Cimento* **9**, 987–998.

Sodha, M.S., Ghatak, A.K. & Tripathi, V.K. (1976). *Progress in Optics* **13**, 169.

Sodha, M.S., Singh, T., Singh, D.P. & Sharma, R.P. (1981). Growth of laser ripple in a plasma and its effect on plasma wave excitation. *Phys. Fluids* **24**, 914–919.

Sodha, M.S., Tewari, D.P. & Subbarao, D. (1983). *Contemporary Plasma Physics*. Delhi, India: Macmillan India Ltd.